

BRIEF COMMUNICATIONS

The purpose of this Brief Communications section is to present important research results of more limited scope than regular articles appearing in *Physics of Fluids A*. Submission of material of a peripheral or cursory nature is strongly discouraged. Brief Communications cannot exceed three printed pages in length, including space allowed for title, figures, tables, references, and an abstract limited to about 100 words.

On the influence of the Basset history force on the motion of a particle through a fluid

P. J. Thomas^{a)}

Deutsche Forschungsanstalt für Luft- und Raumfahrt, Institut für Experimentelle Strömungsmechanik, Bunsenstrasse 10, D-3400 Göttingen, Germany

(Received 27 December 1991; accepted 6 May 1992)

A parameter study on the development of the Basset integral appearing in the equation of motion of a particle moving through a fluid is presented. The particle motion is investigated numerically for the flow across an aerodynamic shock. It is found that, for this type of flow, the Basset history force acting upon the particle described by the Basset integral can be many times larger than the viscous drag in the immediate shock region. It is demonstrated how this force affects the particle motion across the shock for different particles. Nevertheless, the results obtained show that it is justified to neglect the Basset integral for the theoretical description of the motion of the types of particles commonly used in flow measurement tracer techniques for the type of flow considered here.

Measuring techniques like laser Doppler anemometry (LDA) or particle image velocimetry (PIV) rely on the velocity information obtained from micron sized particles transported with a fluid. The ability of these so-called seeding particles to faithfully follow any velocity changes occurring in a flow field is one of the key assumptions of such techniques. This assumption, however, is not necessarily satisfied under the influence of a large velocity gradient.

Under certain assumptions made later on, the motion of a particle through a fluid can be described by the Basset-Boussinesq-Oseen (BBO) equation (see, for instance, Soo¹). The integral term appearing in this equation [Eq. (1)] takes into account deviations of the flow pattern from the steady state. This term is interpreted as an additional flow resistance and is usually referred to as the Basset history integral or Basset integral.

There are numerous publications that numerically study the motion of particles across aerodynamic shocks (e.g., Walsh² and Nichols³). All of these publications account only for the viscous drag acting upon the particle. Nevertheless, it was shown by Hughes and Gilliland⁴ that, in the case of a flow accelerated at high rates, the Basset (history) force, described by the Basset integral, can be many times as large as the stationary viscous drag. Only Tedeschi⁵ discusses the Basset integral for the motion of a particle moving across an aerodynamic shock. He arrives at the conclusion that the Basset force can be neglected for the special case he examined. He does not, on the other hand, show how it actually affects the particle motion.

The purpose of this work is to study the development

of the Basset integral and the influence of the Basset force on the motion of a particle in the presence of a large velocity gradient in greater detail. The study will show how the Basset force affects the particle motion across an aerodynamic shock and it will give stronger support to the common simplification of neglecting the Basset integral when the motion of seeding particles under such flow conditions is considered.

Consider a small (order of size: μm), spherical, nondeformable particle not disturbing the flow. Neglecting wall effects, the motion of that particle in a fluid can be described by the BBO equation, which is given in the notation of Soo¹ as

$$\begin{aligned} \frac{4\pi}{3} r_p^3 \rho_p \frac{d\mathbf{U}_p}{dt_p} = & \frac{4\pi}{3} r_p^3 \rho_p G(\mathbf{U}_F - \mathbf{U}_p) - \frac{4\pi}{3} r_p^3 \frac{\partial P}{\partial \mathbf{r}} \\ & + \frac{1}{2} \frac{4\pi}{3} r_p^3 \rho_F \frac{d}{dt_p} (\mathbf{U}_F - \mathbf{U}_p) \\ & + 6r_p^2 \sqrt{\pi \rho_F \mu_F} \\ & \times \int_{t_{p0}}^{t_p} \frac{(d/d\tau)(\mathbf{U}_F - \mathbf{U}_p)}{\sqrt{t_p - \tau}} d\tau + \mathbf{F}_a \end{aligned} \quad (1)$$

with

$$G = \frac{3}{8} C_D \frac{\rho_F}{\rho_p} \frac{1}{r_p} |\mathbf{U}_F - \mathbf{U}_p|, \quad [\text{sec}^{-1}], \quad (2)$$

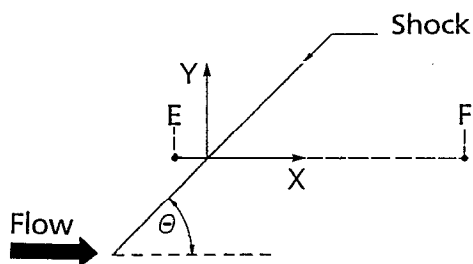


FIG. 1. Oblique shock and measuring traverse \overline{EF} .

where U_p and U_F denote particle and fluid velocity, respectively, and ρ_p , ρ_F are the density of the particle material and the fluid. The radius of the particle is r_p , the viscosity of the fluid is denoted by μ_F , and the empirical drag coefficient of the particle is given by C_D . The physical significance of the five terms on the right-hand side of Eq. (1) is as follows: The first term represents the force acting on the particle due to a stationary viscous flow. The second term is due to the pressure gradient in the surrounding fluid. The third term is referred to as added or apparent mass and represents the force required to accelerate the mass of the fluid surrounding the particle and moving with it; the increment being one-half the mass of the fluid displaced ($1/2 m_F$). The fourth term is the Basset history integral, which was already discussed above. The last term on the right-hand side of Eq. (1) denotes external forces such as gravity.

The pressure term disappears for the flow across an oblique shock in the region of constant downstream flow conditions. It is discussed in Thomas⁶ that it is justified to neglect the added mass term for the type of flow considered. Furthermore, the influence of external forces will be excluded.

The simplified equation of the particle motion across the shock is integrated numerically by the use of the Bulirsch-Stoer method using the routines suggested by Press *et al.*⁷ and the equation for the drag coefficient C_D by Henderson.⁸ The velocity across the shock was modeled as a hyperbolic tangent profile.

With respect to various earlier LDA experiments (e.g., Krishnan *et al.*⁹ and d'Humieres *et al.*¹⁰) in which the flow velocity was measured along a traverse \overline{EF} (Fig. 1), our results are presented in the coordinate system x, y of Fig. 1. Because of the deflection of the flow, a particle detected at any location along \overline{EF} has originally crossed the shock front at a position lying below the intersection of \overline{EF} and the shock front. A transformation of the particle motion into the measuring system of the LDA is obtained by simple geometrical considerations (see Thomas⁶).

The theoretical results presented below refer to the component of the flow velocity in the main flow direction and to the following upstream flow conditions: Mach number $M=1.94$, total pressure $P_0=97\,400$ Pa, static pressure $P_1=13\,650$ Pa, total temperature $T_0=291.4$ K. The shock angle is $\Theta=47.4^\circ$ and a shock thickness of about $7\ \mu\text{m}$ perpendicular to the shock was assumed.

Figures 2(a) and 2(b) show the development of the Basset force and the viscous drag, both per unit mass, across the shock. It can be seen from Fig. 2(a) that, within the shock region, the Basset force starts to increase toward larger negative values farther upstream than the viscous drag. The Basset force takes on its first maximum within the second half of the shock region and starts decreasing rapidly thereafter. The viscous drag reaches its negative maximum slightly farther downstream and decreases then at a slower rate than the Basset force. Figure 2(a) shows that, just downstream of the shock (for $x \gtrsim 10\ \mu\text{m}$), the Basset force is already about one order of magnitude smaller than the viscous drag. Unlike the viscous drag, the Basset force changes its orientation at some location downstream of the shock; this can be seen in Fig. 2(b), where the scale of the ordinate was magnified. The Basset force takes on another maximum at about $x \approx 0.06\ \text{mm}$ and then approaches zero. Figure 3 shows the ratio of the Basset force and the viscous drag in the immediate shock region. It can be seen that, for the largest particle shown ($r_p=2.5$

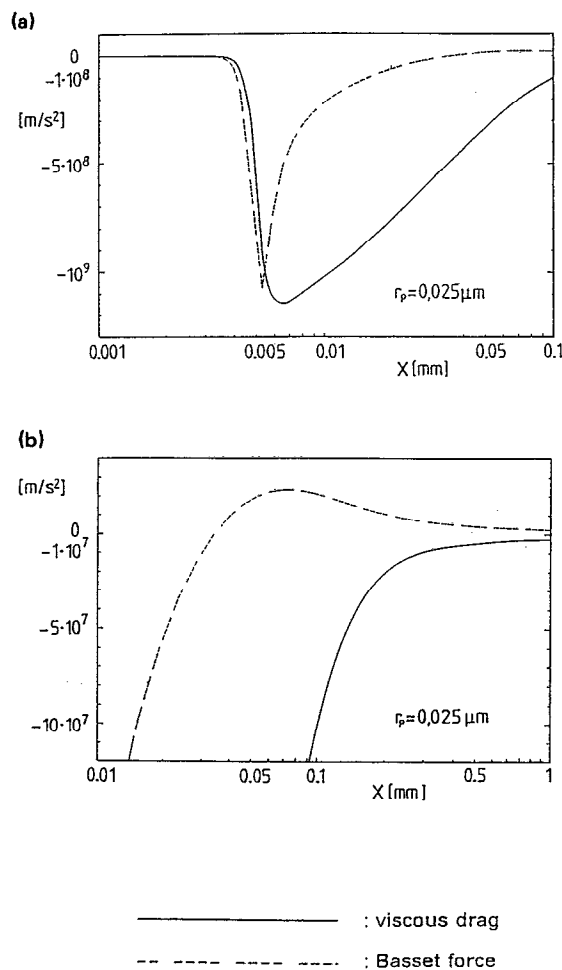


FIG. 2. (a) and (b) show the development of viscous drag and Basset force across the shock ($\rho_p=0.874 \cdot 10^3\ \text{kg/m}^3$).

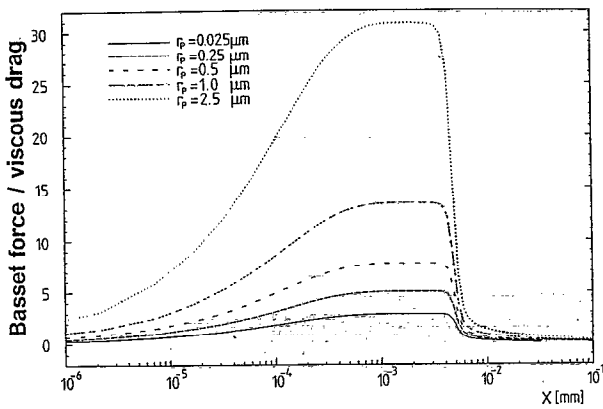
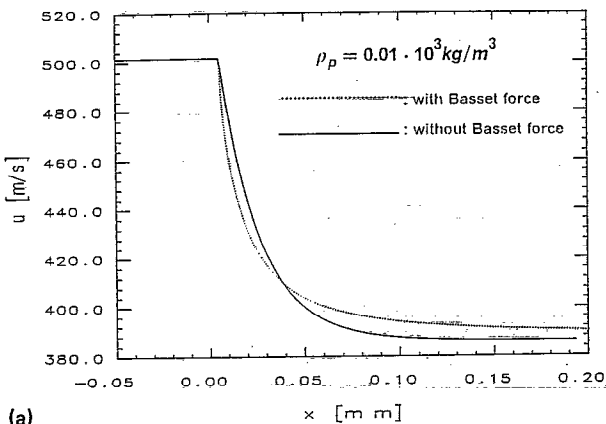


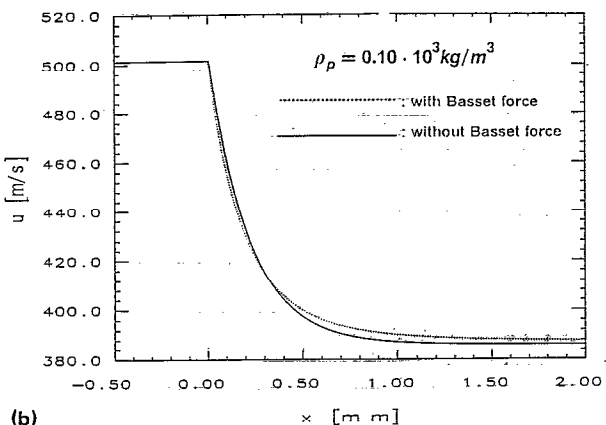
FIG. 3. Ratio of Basset force and viscous drag across the shock.

μm), the Basset force takes on values of up to around 30 times the value of the viscous drag. The ratio decreases with decreasing particle size. All graphs shown in Fig. 3 slope steeply toward the end of the shock region representing the rapid decrease of the Basset force after having taken on its negative maximum [Fig. 2(a)].

The actual influence of the Basset force on the particle motion is shown in Figs. 4(a) and 4(b) for two particles of



(a)



(b)

FIG. 4. (a) and (b) show the influence of the Basset force on the particle motion across the oblique shock, for a particle with a radius of $r_p = 0.5 \mu\text{m}$ and varying density.

different density. From Figs. 4(a) and 4(b), it can be seen how the influence of the Basset force on the particle motion decreases with increasing particle density. Similar curves are obtained for particles of constant density if the particle size is varied, with the influence of the Basset force on the particle motion decreasing for increasing particle size (see Thomas⁶). From Figs. 4(a) and 4(b), it can be seen that the curves obtained, if the Basset force is taken into account or neglected, intersect each other at some location downstream of the shock. This behavior reflects the change of the Basset force's orientation discussed above. Upstream of the point of intersection, the Basset force acts as an additional flow resistance, whereas downstream of this point, its overall effect is a higher particle velocity. Its net effect therefore is an increased relaxation length. The interpretation of the Basset force as an additional flow resistance is thus not entirely correct and is misleading in this case.

The seeding particles commonly used in LDA and other tracer techniques have a radius of around $r_p \approx 0.5 \mu\text{m}$ and a density equal to or higher than approximately $\rho_p \approx 1 \cdot 10^3 \text{ kg/m}^3$. The calculations have shown that the largest difference between the velocity obtained at any location downstream of the shock if the Basset force is neglected or taken into account is of the order of 1–2 m/sec for these particles. This corresponds to 1%–2% relative to the velocity jump across the shock and is of the order of the velocity difference that can be resolved by a LDA. The influence of the Basset force on the particle motion can thus be neglected for tracer technique applications for the type of flow studied here. The Basset force must, on the other hand, be taken into account as is suggested by Figs. 4(a) and 4(b) and further results presented in Thomas⁶ for particles having a radius of around $r_p \approx 0.5 \mu\text{m}$ and a density of $\rho_p \lesssim 0.1 \cdot 10^3 \text{ kg/m}^3$ as well as for particles having a density of $\rho_p \approx 1.0 \cdot 10^3 \text{ kg/m}^3$ and a radius of $r_p \lesssim 0.025 \mu\text{m}$.

¹Present address: Department of Applied Mathematics and Theoretical Physics, University of Cambridge, Silver Street, Cambridge CB3 9EW, England.

²S. L. Soo, *Fluid Dynamics of Multiphase Systems* (Blaisdell, Waltham, MA, 1967).

³M. J. Walsh, "Influence of particle drag coefficient on particle motion in high-speed flow with typical laser velocimeter applications," NASA Tech. Note TND-8120, 1976.

⁴R. H. Nichols, "Calculation of particle dynamics effects on laser velocimeter data," in *Wind Tunnel Seeding Systems for Laser Velocimeters*, NASA Conf. Publ. 2393. Workshop at Langley Research Center 19–20 September 1985.

⁵R. R. Hughes and E. R. Gilliland, "The mechanics of drops," *Chem. Eng. Prog.* **48**, 497 (1952).

⁶G. Tedeschi, "Analyse Théorique du comportement de particules relativement à la traversée d'un onde de choc," Diplôme d'études approfondies de mécanique des Fluides, L'Université D'Aix-Marseille II, Institut de Mécanique statistique de la Turbulence, Marseille, France, 1989.

⁷P. Thomas, "Experimentelle und theoretische Untersuchungen zum Folgerverhalten von Teilchen unter dem Einfluss grosser Geschwindigkeitsgradienten in kompressibler Strömung," Deutsche Forschungsanstalt für Luft- und Raumfahrt, Germany, Research Report No. DLR-FB 91-25, 1991.

- ⁷H. W. Press, B. P. Flannery, S. A. Teukolsky, and W. T. Vetterling, *Numerical Recipes* (Cambridge U. P., Cambridge, England, 1986).
- ⁸C. B. Henderson, "Drag coefficients of spheres in continuum and rarefied flows," *AIAA J.* **14**, 707 (1976).
- ⁹V. Krishnan, K.-A. Bütefisch, and K.-H. Sauerland, "Velocity and turbulence measurements in the shock region using the two component laser Doppler anemometer," in *Proceedings of ICALEO 1987*, Vol. 63, Optical Methods in Flow & Particle Diagnostics, edited by W. H. Stevenson (1987).
- ¹⁰C. d'Humieres, F. Micheli, and O. Papirnyk, "Etude du comportement des Aerosols pour la Mesure en Velocimetrie Laser," in *Actes du 2 ème Congres Franco phone de Velocimetrie Laser*, ONERA, Meudon, France, 25-27 September 1990.